Effects on the Seismic Structural Response Spectra From Numerical Model of Structure and Site Model

Xiaoying Sun & Jian Chen
China Nuclear Power Engineering Co., Ltd.

SUMMARY
In the seismic analysis for Category Ⅰ structures of nuclear power plants in China, lumped mass stick models are generally used when calculating the floor response spectra, but the site nonlinearity is not usually considered. These operations, however, may lead to over-conservative, or sometimes underestimated, results which will further affect the designs of the structures and equipments. In this article, the effects on the floor response spectra from the numerical model of structure and the site model were studied. A reactor building's internal structure of a Chinese nuclear power plant was taken as example. The study considers such cases: i) for the structure, considering a reactor building as a three-dimensional finite element model and a lumped mass stick model; ii) for the site, considering linear and nonlinear (equivalent linear) site response respectively. For all these cases, the site property parameters and the input control motion were kept unchanged. The floor response spectra of the internal structure, in each case, were calculated and analyzed by using the 3D finite element program ACS SASSI. Based on the analysis, the effects on the floor response spectra from the two numerical models of a structure and the different site models were discussed.

Keywords: Equivalent linear, Floor response spectrum, SSI

1. INTRODUCTION

Nuclear power plays an important and special role in fields of energy construction, military scientific research and technology development. Nuclear power research, in many countries, has been one of the top scientific researching subjects. One biggest danger from nuclear power plants is that it may cause serious harms to human health and the natural environments once the massive radioactive materials in the nuclear power plants leak out. Therefore, countries located at active tectonic region, like Japan, USA and China, concentrate much on the seismic safety of nuclear power plants. In a nuclear power plant, the most important structure to prevent the leakage of radioactive materials is the reactor building (RB). According to Standard Review Plan (U.S.NRC, 2007), RB is classified as a Seismic Category Ⅰ building. In a RB, the internal structure accommodates and supports the key equipments and pipes of the primary circuit. The seismic design of the internal structure of RB is considerably complicated due to the complexity of the internal structure.

The seismic analysis technique of nuclear power plants (NPP) is comparably advanced in some developed countries like USA and French due to their long histories of nuclear power plant construction and research. With the aid of high performance computers, present seismic analyses of NPP structures can consider the effects from site-structure interaction (SSI), site nonlinearity, numerical model of structure, and incoherency of input motions. Some researches can even consider two or three of those effects in one case (Ghiocel *et al*, 2009; LI *et al*, 2010; LIN, 2011; PEI *et al*, 2011). By contrast, the seismic analysis technology for nuclear power plants in China is not as advanced as that in those developed countries. The NPP buildings are always simplified as lumped mass stick models, and the consideration of site nonlinearity is always ignored since most NPP structures in China are built on rock foundations.

In this paper, the effects of numerical model of structure and site model on the floor response spectra were investigated. For the investigation, the seismic analysis of a real RB's internal structure of an in-service pressurized-water reactor NPP was performed by using program ACS SASSI and ANSYS. The analysis considers five different site condition cases. For all these cases, the SSI effect was considered. The results of this paper can be used as a reference to current seismic research of nuclear power engineering in China.

2. PARAMETERS

The internal structure, consisting of thick walls and thick floor slabs, is a complicated building with the radius of about 21m and the height of about 39m. Fig. 2.1 and 2.2 are the plan view and vertical view of the internal structure respectively. The thick walls have several different types including cylindrical walls arranged radially and straight walls arranged with a certain angle between its longitudinal centre line and X-axis (see Fig. 2.1 to Fig. 2.3). There also have the axis deviation between some adjacent walls, the large openings on some floor slabs, and staggered floors. All these factors make the seismic analysis of the internal structure more complicated.

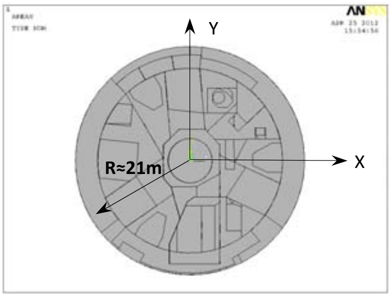

Figure 2.1. Plan view of the internal structure

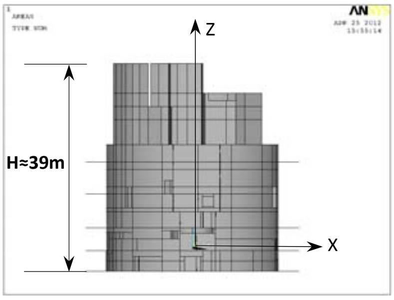

Figure 2.2. Vertical view of the internal structure

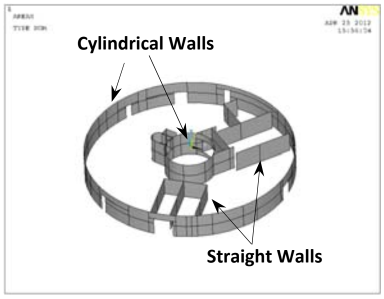

Figure 2.3. Cylindrical walls and straight walls

2.1. Numerical Model of Structure

Two numerical models are used: a three-dimensional finite element model (3D model for short) founded from program ANSYS (Fig. 2.4) and a lumped mass stick model (stick model for short, see Fig. 2.5). In the 3D model, the walls and floor slabs are modeled using thick shell element SHELL181 and the mass of the equipments are modeled by mass element MASS21.

The stick model is obtained by simplifying the 3D model following the principles below: 1) The elevation of the main floor's centroid in the 3D model is defined to be the elevation of the lumped mass in the stick model; 2) The lumped mass at a certain elevation in the stick model includes the following masses in the 3D model: the masses of the floors at the corresponding elevation, the masses of the equipments on the floors, and one half of the masses of the walls which are connected to the floors; 3) The parameters of the walls between two adjacent floors, including cross-sectional area, shear area, inertia moment and rotary inertia, computed based on mechanical principles, are defined to be the dynamic properties of the connection sticks between the lumped masses.

The floors at the elevation +4.65m, +10.20m and +19.11m support the key equipments and the pipes of the primary circuit, so only the response spectra at the three elevations are output for comparison. Particularly, in the 3D model, the response spectrum at a certain elevation is obtained by enveloping the response spectra of all nodes at the elevation.

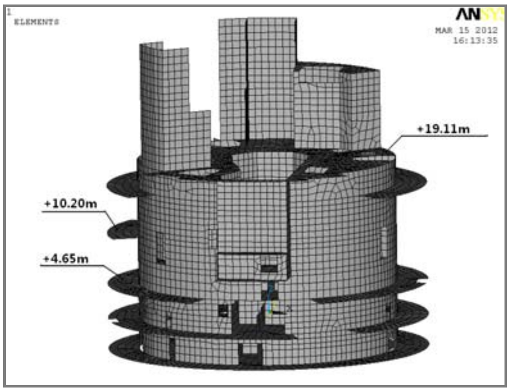

Figure 2.4. 3D finite element model

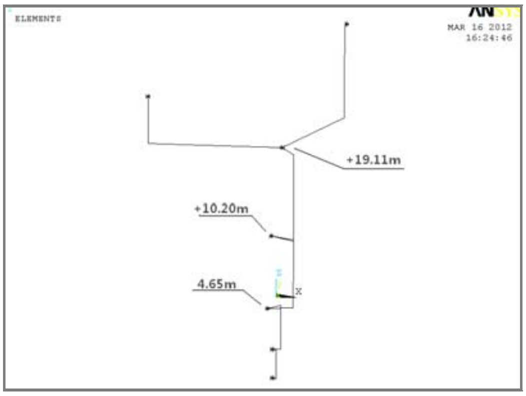

Figure 2.5. Lumped mass stick model

2.2. Site Conditions

With reference to the foundation parameters of some in-service, under-construction and perspective nuclear power plants in China, we consider five site conditions in the study. The parameters of the five site conditions are listed in Table 2.1. According to Standard Review Plan (U.S.NRC, 2007) , "*For structures founded on materials having a shear wave velocity of 8,000 feet per second or higher, under the entire surface of the foundation, a fixed base assumption is acceptable*", the maximum shear wave velocity is taken to be 2400m/s (8000ft/s).

Table 2.1. Dynamic Parameters of the Site Conditions

Site conditions	Unit Density (N/m^3)	Shear Wave Velocity Vs (m/s)	Damping Ratio	Shear Modulus G (MPa)	Poisson Ratio
S1	19621	398	0.06	3180	0.42
S2	21582	699	0.05	10749	0.37
S3	23054	1099	0.04	28383	0.36
S4	25506	1729	0.02	77725	0.30
S5	26487	2400	0.03	155520	0.28

2.3. Input Motions

Following the provisions in Standard Review Plan (U.S.NRC, 2007), the input time history is obtained from the fit to the target spectrum RG 1.60 (U.S.AEC, 1973) with a real accelerogram as seed. The total duration of the time history is 40.96 seconds, the stationary phase strong-motion duration is 10 seconds, and the peak acceleration is 0.3g. The obtained time history shown in Fig. 2.6 is in horizontal direction (X-direction see Fig. 2.1) and the one shown in Fig. 2.7 is in vertical direction (Z-direction see Fig. 2.2). The correlation coefficient of the two input time histories is less than 0.16. The acceleration time histories are input at the foundation bottom elevation.

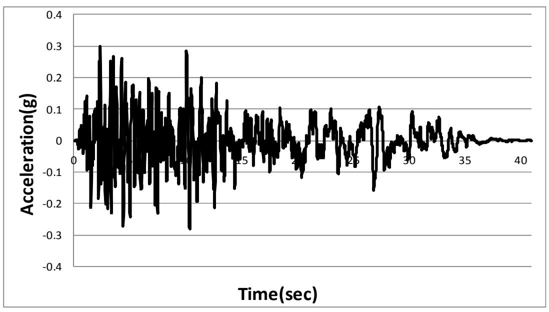

Figure 2.6. X-direction time history

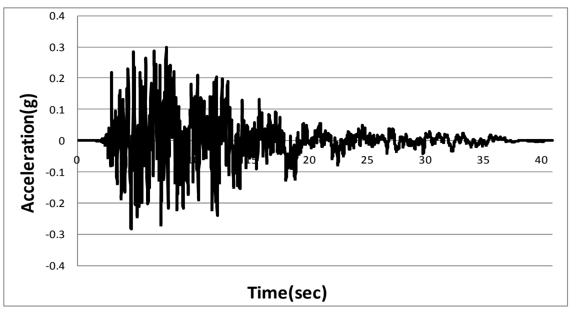

Figure 2.7. Z-direction time history

2.4. Analysis Programs

The programs ACS SASSI V2.3.0 and ANSYS 10.0 are used. ACS SASSI is used to calculate the floor response spectra and ANSYS is used to build the 3D numerical model of the structure. ACS SASSI is a state-of-the-art highly specialized finite element computer code for performing 3D nonlinear site-structure interaction (SSI) analyses for shallow, embedded, deeply embedded and buried structures under coherent and incoherent earthquake ground motions (ACS SASSI User Manuals, 2009).

3. SCHEMES

Two cases are studied: **Case Ⅰ** is to investigate the effect of the numerical model of structure (the 3D model and the stick model) on the response spectra for the five site conditions; **Case Ⅱ** is to investigate the effect of site model (the linear site model and the equivalent linear site model) on the response spectra for the five site conditions.

In Case Ⅰ, a linear site model is used, and the SSI effect is considered. For each numerical model of structure, the 2%-damp floor response spectra in both X- and Z-direction at elevation +4.65m, +10.20m and +19.11m are calculated for comparison.

In Case Ⅱ, only the 3D model of structure is used, and the SSI effect is also considered. For each site model, the 2%-damp floor response spectra in both X- and Z-directions at elevation +4.65m, +10.20m and +19.11m are calculated for comparison. The site deposit is simplified as a 10 horizontal layers of infinite extent. The equivalent linear site model is obtained from the eight times iteration with the initial linear parameters shown in Table 2.1, by using module SITE of ACS SASSI. Fig. 3.1 shows the linear site model for S1 site condition, Fig. 3.2 and 3.3 show the equivalent linear models for S1 site condition corresponding to X- and Z-direction input motions, respectively.

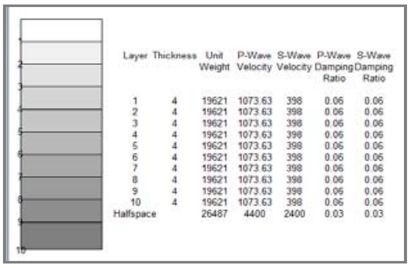

Layer	Thickness	Unit Weight	P-Wave Velocity	S-Wave Velocity	P-Wave Damping Ratio	S-Wave Damping Ratio
1	4	19621	1073.63	398	0.06	0.06
2	4	19621	1073.63	398	0.06	0.06
3	4	19621	1073.63	398	0.06	0.06
4	4	19621	1073.63	398	0.06	0.06
5	4	19621	1073.63	398	0.06	0.06
6	4	19621	1073.63	398	0.06	0.06
7	4	19621	1073.63	398	0.06	0.06
8	4	19621	1073.63	398	0.06	0.06
9	4	19621	1073.63	398	0.06	0.06
10	4	19621	1073.63	398	0.06	0.06
Halfspace		26487	4400	2400	0.03	0.03

Figure 3.1. Linear model for S1 site condition

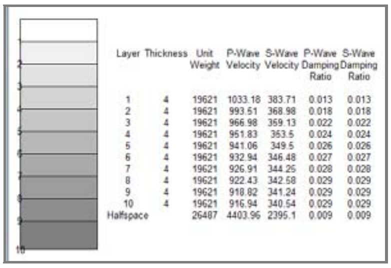

Layer	Thickness	Unit Weight	P-Wave Velocity	S-Wave Velocity	P-Wave Damping Ratio	S-Wave Damping Ratio
1	4	19621	1033.18	383.71	0.013	0.013
2	4	19621	993.51	368.98	0.018	0.018
3	4	19621	966.98	359.13	0.022	0.022
4	4	19621	951.83	353.5	0.024	0.024
5	4	19621	941.06	349.5	0.026	0.026
6	4	19621	932.94	346.48	0.027	0.027
7	4	19621	926.91	344.25	0.028	0.028
8	4	19621	922.43	342.58	0.029	0.029
9	4	19621	918.82	341.24	0.029	0.029
10	4	19621	916.94	340.54	0.029	0.029
Halfspace		26487	4403.96	2395.1	0.009	0.009

Figure 3.2. Equivalent linear model for S1 site condition for X-direction input motion

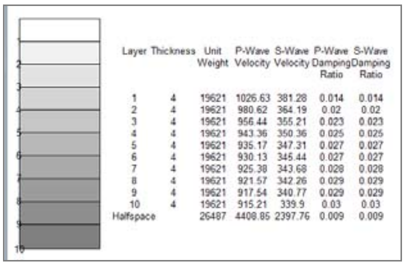

Layer	Thickness	Unit Weight	P-Wave Velocity	S-Wave Velocity	P-Wave Damping Ratio	S-Wave Damping Ratio
1	4	19621	1026.63	381.28	0.014	0.014
2	4	19621	980.62	364.19	0.02	0.02
3	4	19621	956.44	355.21	0.023	0.023
4	4	19621	943.36	350.36	0.025	0.025
5	4	19621	935.17	347.31	0.027	0.027
6	4	19621	930.13	345.44	0.027	0.027
7	4	19621	925.38	343.68	0.028	0.028
8	4	19621	921.57	342.26	0.029	0.029
9	4	19621	917.54	340.77	0.029	0.029
10	4	19621	915.21	339.9	0.03	0.03
Halfspace		26487	4408.85	2397.76	0.009	0.009

Figure 3.3. Equivalent linear model for S1 site condition for Z-direction input motion

4. RESULTS

4.1. Case Ⅰ

The 2%-damp floor response spectra from the 3D model and the stick model for different site conditions, elevations are shown in Fig. 4.1 to 4.6, in which Fig. 4.1 to 4.3 are for X-direction and Fig. 4.4 to 4.6 are for Z-direction. The peak spectral accelerations, the corresponding frequencies, and the zero period accelerations (ZPA) of these response spectra (RS) are listed in Table 4.1.

It can be seen from the table and the figures that: 1) Peak frequency: for X-direction, the peak frequencies from the 3D model are always lower than those from the stick model, and the difference between the peak frequencies become larger as the stiffness of the site condition increases; for Z-direction, the peak frequencies from the two numerical models are nearly identical; 2) Peak spectral acceleration: for X-direction, the peak spectral accelerations from the 3D model are generally larger than those from the stick model, and the difference become smaller as the site condition's stiffness increases; for Z-direction, the peak spectral accelerations from the 3D model are always larger than those from the stick model. The larger the site condition's stiffness, the larger difference between the peak spectral accelerations from the two models. The maximum difference is up to 84.10%; 3) ZPA: for X-direction, the ZPA from the 3D model are generally larger than those from the stick model, and the difference decreases with the increase of the stiffness of the site conditions; for Z-direction, the ZPA from the 3D model are always larger than those from the stick model. The higher shear wave velocity, the larger difference. The maximum difference is up to 66.25%.

The difference between the results from the two numerical models is most likely due to the "rigid floor" assumption used to build the stick model from the 3D model. Actually, there are many openings on the floor slabs at elevation +4.65m, +10.20m and +19.11m. Especially at the +10.20m floor, the sum of these openings' areas exceeds 60% of the total area. These openings will significantly reduce the slabs' stiffness. However, when using the simplifying principles to get the stick model, the floor slabs are assumed to be infinitely rigid to ensure the transmission of the member force. This "rigid floor" assumption will lead to a certain extent error of the vibration modes and the natural frequencies of the structure to the fact. As listed in Table 4.2, the natural frequencies of the 3D model and the stick model have a certain difference. For X-direction, the natural frequencies of the 3D model are lower than those of the stick model, which can be observed from Fig. 4.1 to 4.3. For Z-direction, the natural frequencies of the two numerical models are much closed, but using the 3D model causes larger response because of the larger flexibility of the slabs in the 3D model.

Table 4.1. Floor Response Spectra Computed by Using the 3D Model and the Stick Model

			Peak Frequency(Hz)			Peak Spectral Acceleration(g)			ZPA(g)		
			3D	stick	Offset (3D-stick)	3D	stick	Δ	3D	stick	Δ
4.65m	X	S1	2.524	2.524	0	2.333	2.077	10.98%	0.408	0.380	6.94%
		S2	4.553	5.416	-0.863	2.889	2.336	19.16%	0.457	0.398	12.95%
		S3	5.805	7.149	-1.344	4.033	2.994	25.76%	0.479	0.503	5.14%
		S4	7.149	8.504	-1.355	3.987	3.711	6.92%	0.567	0.516	8.98%
		S5	7.149	8.805	-1.656	4.439	3.823	13.87%	0.572	0.498	12.92%
	Z	S1	3.697	3.697	0	3.143	2.604	17.15%	0.502	0.360	28.36%
		S2	6.442	6.442	0	2.626	2.022	23.00%	0.574	0.391	31.93%
		S3	9.771	9.116	0.655	3.141	2.058	34.48%	0.567	0.403	28.91%
		S4	10.844	10.844	0	3.376	1.750	48.16%	0.758	0.390	48.54%
		S5	17.028	17.028	0	5.977	1.527	74.45%	0.860	0.385	55.23%
10.20m	X	S1	3.697	4.103	-0.406	2.654	2.345	11.61%	0.482	0.427	11.27%
		S2	5.416	6.01	-0.594	3.649	2.903	20.44%	0.558	0.438	21.43%
		S3	6.01	7.663	-1.653	5.226	4.054	22.42%	0.672	0.608	9.45%
		S4	7.149	8.504	-1.355	5.500	5.514	-0.25%	0.721	0.631	12.36%
		S5	7.149	8.805	-1.656	6.013	5.691	5.35%	0.710	0.641	9.78%
	Z	S1	3.697	3.697	0	3.130	2.623	16.22%	0.412	0.366	11.30%
		S2	6.67	6.67	0	2.784	2.232	19.84%	0.452	0.395	12.65%
		S3	9.116	9.116	0	2.946	2.125	27.87%	0.479	0.412	14.15%
		S4	10.844	10.844	0	2.526	1.843	27.04%	0.578	0.414	28.27%
		S5	15.886	17.028	-1.142	2.670	1.776	33.51%	0.589	0.414	29.75%
19.11m	X	S1	3.697	4.103	-0.406	3.400	3.024	11.06%	0.584	0.480	17.73%
		S2	5.416	6.223	-0.807	4.868	3.697	24.05%	0.705	0.560	20.53%
		S3	6.01	7.663	-1.653	6.808	5.477	19.55%	0.917	0.755	17.68%
		S4	7.149	8.504	-1.355	7.442	7.658	-2.91%	0.949	0.849	10.49%
		S5	7.149	8.805	-1.656	7.934	7.964	-0.37%	0.909	0.880	3.20%
	Z	S1	3.697	3.697	0	3.204	2.630	17.91%	0.582	0.369	36.53%
		S2	6.67	6.67	0	3.176	2.256	28.97%	0.723	0.398	44.85%
		S3	9.116	9.116	0	4.036	2.173	46.16%	0.657	0.417	36.61%
		S4	10.844	10.844	0	4.362	1.909	56.24%	1.078	0.434	59.74%
		S5	17.028	17.028	0	12.223	1.943	84.10%	1.289	0.435	66.25%

Note: Δ=($Acceleration_{3D}$- $Acceleration_{stick}$)/ $Acceleration_{3D}$

Table 4.2. Natural Frequencies of the 3D Model and the Stick Model

Mode	3D model (Hz)	Stick model (Hz)	Direction
1	8.063	9.867	X
2	16.231	20.577	Z
3	16.516	21.243	Z
4	17.243	23.673	Z

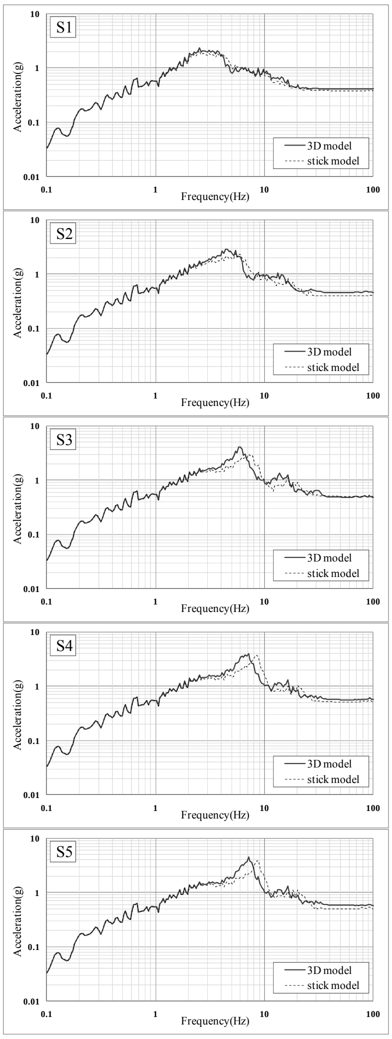

Figure 4.1. 2%-Damp RS of El. 4.65m for X-direction:
3D Model vs. Stick Model

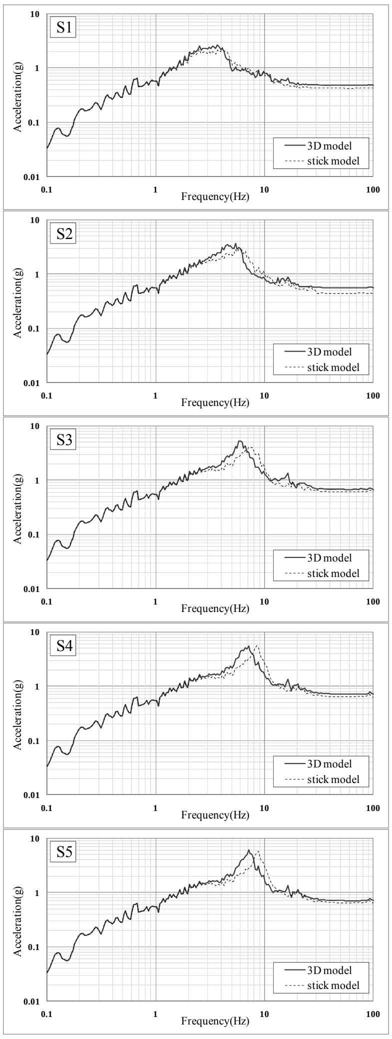

Figure 4.2. 2%-Damp RS of El. 10.20m for X-direction:
3D Model vs. Stick Model

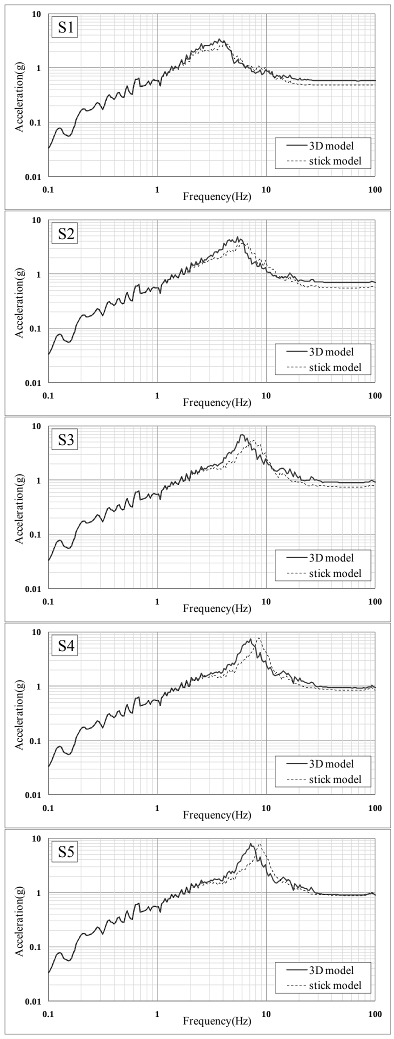

Figure 4.3. 2%-Damp RS of El. 19.11m for X-direction:
3D Model vs. Stick Model

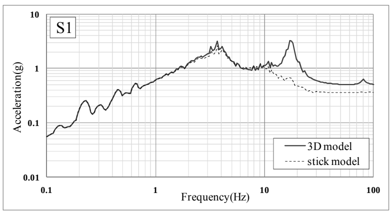

Figure 4.4. 2%-Damp RS of El. 4.65m for Z-direction:
3D Model vs. Stick Model

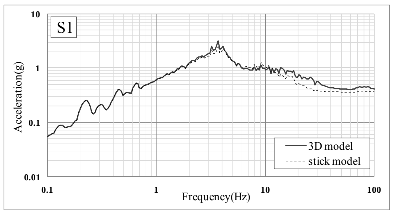

Figure 4.5. 2%-Damp RS of El. 10.20m for Z-direction:
3D Model vs. Stick Model

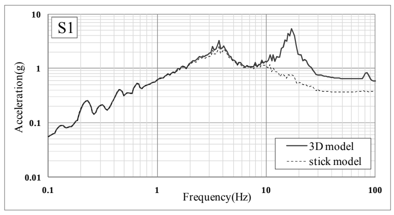

Figure 4.6. 2%-Damp RS of El. 19.11m for Z-direction:
3D Model vs. Stick Model

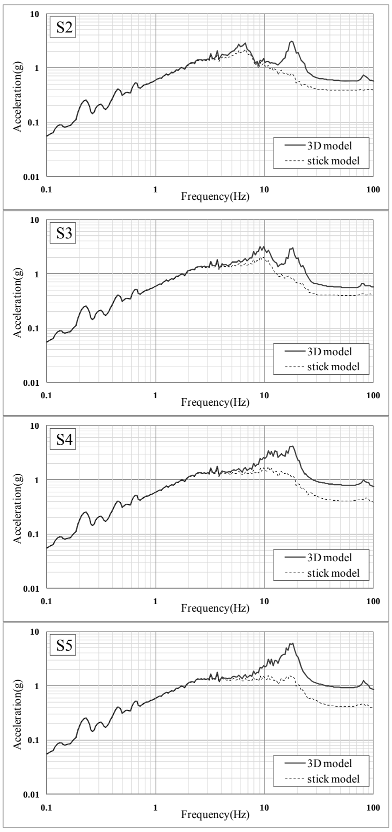

Figure 4.4 (cont.) 2%-Damp RS of El. 4.65m for Z-direction: 3D Model vs. Stick Model

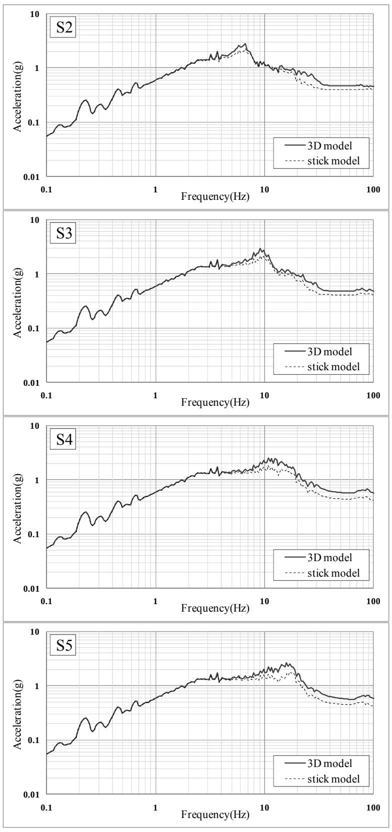

Figure 4.5 (cont.) 2%-Damp RS of El. 10.20m for Z-direction: 3D Model vs. Stick Model

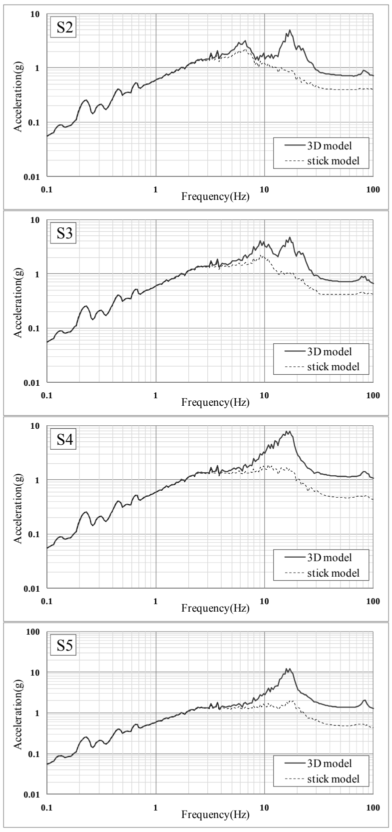

Figure 4.6 (cont.) 2%-Damp RS of El. 19.11m for Z-direction: 3D Model vs. Stick Model

4.2 Case Ⅱ

The 2%-damp floor response spectra from the linear site model and the equivalent linear site model for different site conditions, elevations are shown from Fig. 4.7 to 4.12, in which Fig. 4.7 to 4.9 are for X-direction and Fig. 4.10 to 4.12 are for Z-direction. The peak spectral accelerations, the corresponding frequencies, and the ZPA of these response spectra are listed in Table 4.3.

It can be seen from the table and the figures that: 1) Peak frequency: for X-direction, the difference between the peak frequencies from using linear site model and from using equivalent linear site model is not large, and the higher elevation, the smaller difference; for Z-direction, the peak frequencies from using the two site models for all site conditions are much close except for the S1 site condition in which a difference of 1.142Hz appears; 2) Peak spectral acceleration: for both X- and Z-direction, the peak spectral accelerations from using the linear site model are larger than those from using the equivalent linear site model. The maximum difference for S1 site condition (Vs=398m/s) is 25.42%. For all other four site conditions, the differences between the peak spectral accelerations from using the two models are not large, and the maximum difference is up to 10.89% appeared in S3 site condition (Vs=1099m/s); 3) ZPA: for both X- and Z-direction, the ZPA from using the linear site model are smaller than those from using the equivalent linear site model, and the difference of the ZPA decreases as the stiffness of the foundation increases. The maximum difference up to 27.25% appears in S1 site condition. The difference of the ZPA for S2 site condition has a maximum of 9.36%. For the other three site conditions, the differences are always within 5%.

In a word, using linear or equivalent linear site model has only a little effect on the floor response spectra. However, this effect is usually more significant in X-direction than in Z-direction, and is more significant for softer foundation than harder foundation.

Table 4.3. RS Computed by Using Linear Site Model and Equivalent Linear Site Model

			Peak Frequency(Hz)			Peak Spectral Acceleration(g)			ZPA(g)		
			Linear	EQlinear	Offset (Linear-EQlinear)	Linear	EQlinear	Δ	Linear	EQlinear	Δ
4.65m	X	S1	2.524	3.002	-0.479	2.333	2.202	5.64%	0.408	0.414	-1.38%
		S2	4.553	4.553	0	2.889	2.983	-3.25%	0.457	0.466	-1.93%
		S3	6.01	5.805	0.205	4.033	4.384	-8.72%	0.479	0.513	-7.17%
		S4	7.149	7.149	0	3.987	4.077	-2.26%	0.567	0.574	-1.27%
		S5	7.149	7.149	0	4.439	4.567	-2.87%	0.572	0.579	-1.27%
	Z	S1	3.697	3.218	0.479	3.143	3.240	-9.70%	0.502	0.599	-19.27%
		S2	6.67	5.805	0	2.848	3.009	-5.65%	0.574	0.627	-9.36%
		S3	9.771	9.116	0.655	3.141	3.456	-10.02%	0.567	0.593	-4.51%
		S4	18.252	18.252	0	4.195	4.162	0.80%	0.758	0.759	-0.03%
		S5	18.252	18.252	0	6.011	6.042	-0.52%	0.860	0.865	-0.67%
10.20m	X	S1	3.697	3.331	0.366	2.654	2.863	-7.87%	0.482	0.500	-3.87%
		S2	5.416	5.416	0	3.649	3.843	-5.32%	0.558	0.576	-3.32%
		S3	6.01	6.01	0	5.226	5.732	-9.68%	0.672	0.702	-4.51%
		S4	7.149	7.149	0	5.500	5.643	-2.60%	0.721	0.734	-1.81%
		S5	7.149	7.149	0	6.013	6.192	-2.98%	0.710	0.720	-1.39%
	Z	S1	3.697	3.218	0.479	3.130	3.224	-3.00%	0.412	0.459	-11.45%
		S2	6.67	5.805	0.865	2.784	2.939	-5.56%	0.452	0.492	-8.93%
		S3	9.116	9.116	0	2.946	3.267	-10.89%	0.479	0.499	-4.17%
		S4	10.844	10.844	0	2.526	2.555	-1.14%	0.578	0.578	-0.15%
		S5	15.886	15.886	0	2.670	2.718	-1.79%	0.589	0.592	-0.57%
19.11m	X	S1	3.697	3.571	0.126	3.400	3.732	-9.79%	0.584	0.607	-3.94%
		S2	5.416	5.416	0	4.868	5.175	-6.30%	0.705	0.734	-4.17%
		S3	6.01	6.01	0	6.808	7.516	-10.40%	0.917	0.960	-4.71%
		S4	7.149	7.149	0	7.442	7.633	-2.57%	0.949	0.966	-1.85%
		S5	7.149	7.149	0	7.934	8.169	-2.96%	0.909	0.925	-1.82%
	Z	S1	17.028	15.886	1.142	5.347	3.988	25.42%	0.582	0.740	-27.25%
		S2	17.028	17.028	0	4.949	4.710	4.82%	0.723	0.789	-9.24%
		S3	17.028	17.028	0	4.688	4.673	0.31%	0.657	0.686	-4.43%
		S4	17.028	17.028	0	7.846	7.740	1.35%	1.078	1.076	0.24%
		S5	17.028	17.028	0	12.223	12.392	-1.38%	1.289	1.310	-1.58%

Note: $\Delta=(\text{Acceleration}_{linear}-\text{Acceleration}_{eqlinear})/\text{Acceleration}_{linear}$

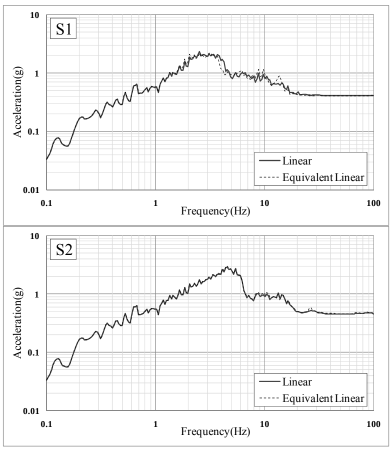

Figure 4.7. 2%-Damp RS of El. 4.65m for X-direction:
Linear vs. Equivalent Linear

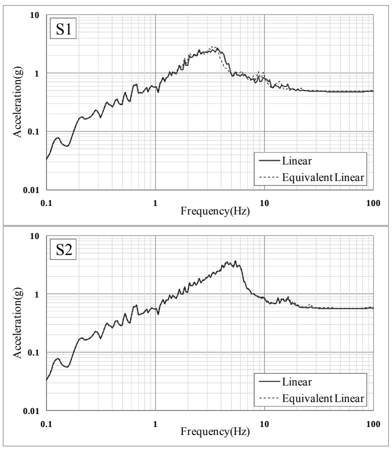

Figure 4.8. 2%-Damp RS of El. 10.20m for X-direction:
Linear vs. Equivalent Linear

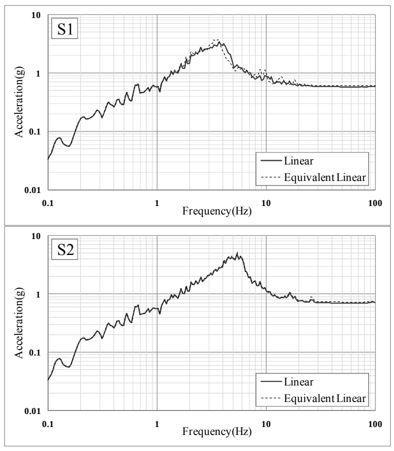

Figure 4.9. 2%-Damp RS of El. 19.11m for X-direction:
Linear vs. Equivalent Linear

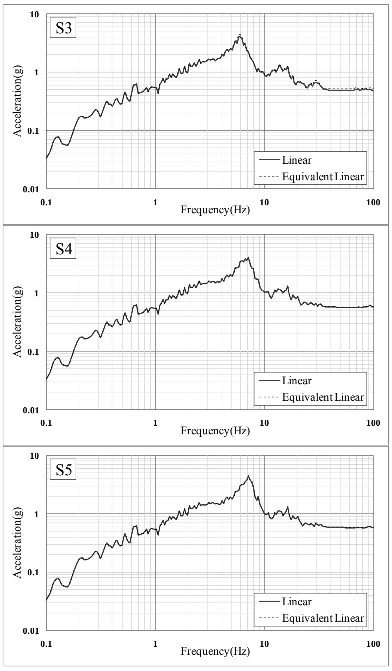

Figure 4.7 (cont.) 2%-Damp RS of El. 4.65m for X-direction: Linear vs. Equivalent Linear

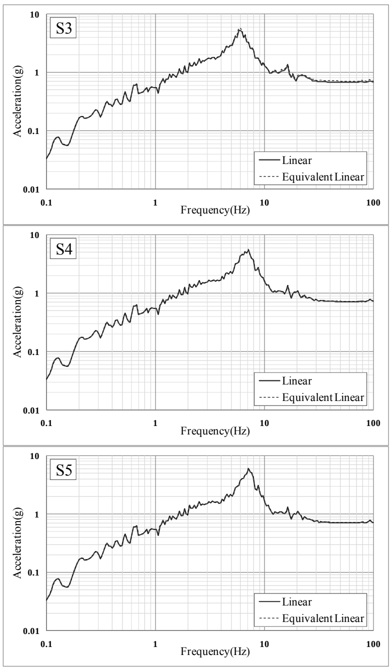

Figure 4.8 (cont.) 2%-Damp RS of El. 10.20m for X-direction: Linear vs. Equivalent Linear

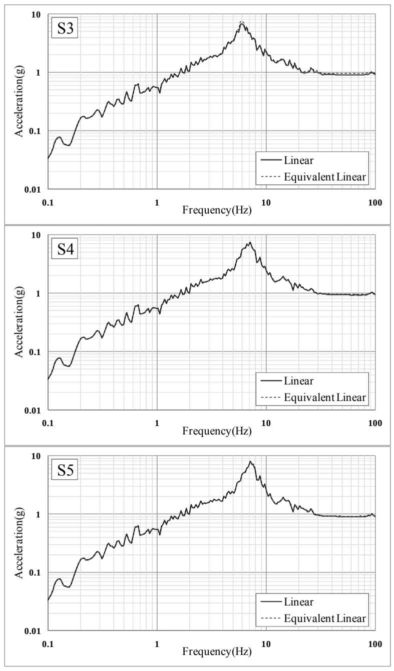

Figure 4.9 (cont.) 2%-Damp RS of El. 19.11m for X-direction: Linear vs. Equivalent Linear

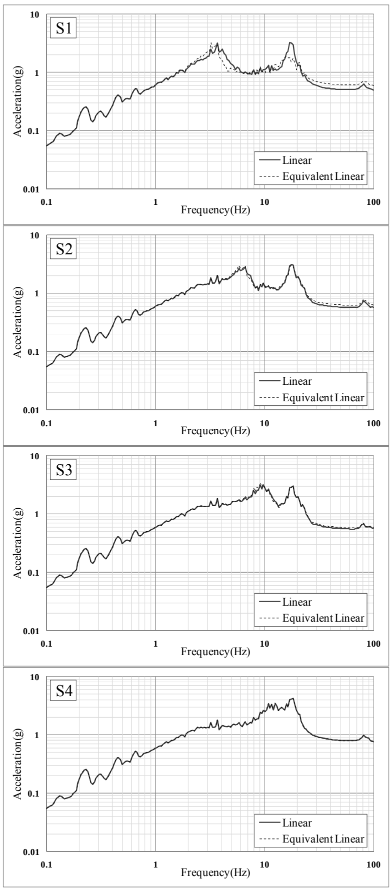

Figure 4.10. 2%-Damp RS of El. 4.65m for Z-direction: Linear vs. Equivalent Linear

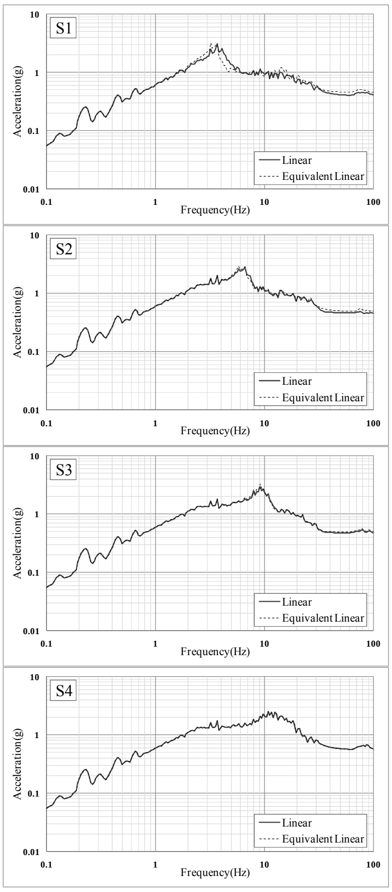

Figure 4.11. 2%-Damp RS of El. 10.20m for Z-direction: Linear vs. Equivalent Linear

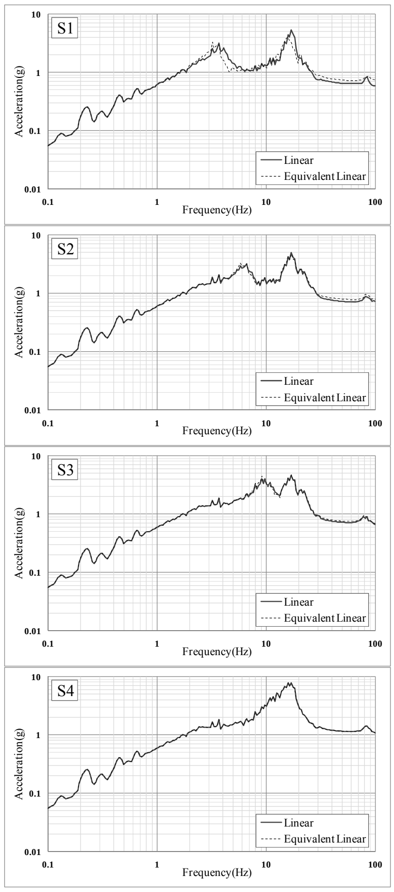

Figure 4.12. 2%-Damp RS of El. 19.11m for Z-direction: Linear vs. Equivalent Linear

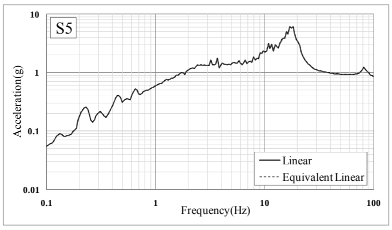

Figure 4.10 (cont.) 2%-Damp RS of El. 4.65m for Z-direction: Linear vs. Equivalent Linear

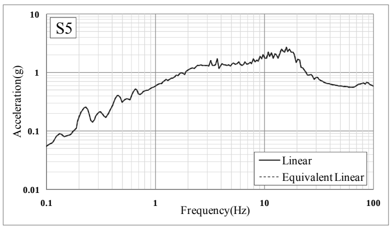

Figure 4.11 (cont.) 2%-Damp RS of El. 10.20m for Z-direction: Linear vs. Equivalent Linear

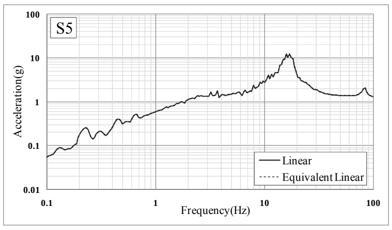

Figure 4.12 (cont.) 2%-Damp RS of El. 19.11m for Z-direction: Linear vs. Equivalent Linear

5. CONCLUSION

In this article, the seismic analysis of the internal structure of an in-service nuclear power plant in China was performed, in which the effects on the floor response spectrum from the numerical model of structure and the site model were studied. The study led to the following conclusions: 1) Using 3D model or lumped mass stick model has a significant effect on the floor response spectra of the internal structure. For X-direction, the peak spectral accelerations from using 3D model are generally larger than those from using stick model, and the difference of the peak spectral accelerations decreases as the stiffness of the site condition increases. The peak frequencies of the floor response spectra from using 3D model is always smaller than those from using stick model; For Z-direction, the peak frequencies of the floor response spectra from using the two different models are much closed, but the peak spectral accelerations have a difference up to 84.10%. The results show the importance of using 3D finite element model to replace the lumped mass stick model in the seismic analysis of the internal structure; 2) Using linear or equivalent linear site model has only a little effect on the floor response spectra, and this effect is observable only when the shear wave velocity of the foundation is lower than 700m/s. When the shear wave velocity exceeds 1100m/s, the effect of the adopted site model can be negligible.

ACKNOWLEDGEMENT
The authors thank professor senior engineer Zhang Chaoqi, the vice chief engineer of CNPE, for her valuable instructions and suggestions. We are also grateful to Dr. Sun Xiaodan and professor senior engineer Lu Fei for their great help on the writing of the manuscript.

REFERENCES

Dan M. Ghiocel, Stephen Short and Greg Hardy (2009). Seismic Motion Incoherency Effects on SSI Response of Nuclear Islands with Significant Mass Eccentricities and Different Embedment Levels. *20th International Conference on Structural Mechanics in Reactor Technology*. **SMiRT 20-Division K,** Paper 1852**.**

Dan M. Ghiocel, Dali Li and Keith Coogler (2009). Seismic Motion Incoherency Effects for AP1000 Nuclear Island Complex. *20th International Conference on Structural Mechanics in Reactor Technology*. **SMiRT 20-Division K,** Paper 1853**.**

Ghiocel Predictive Technologies, Inc., (2009). ACS SASSI NQA Version 2.3.0 User Manuals, USA

LI Jian-bo, LIN Gao and ZHU Xiu-yun (2010).Study on Ground Numerical Models for Flooor Response Spectra Analysis of Nuclear Power Plant and Their Influences.*Nuclear Power Engineering***31:4**,91-95.

LIN Gao (2011). Review on seismic design of nuclear power project(II). *Yangtze River***42:21**, 1-6.

PEI Qiang, XUE Zhicheng and HU Bo (2011). Seismic response analysis of nuclear reactor buildings considering inhomogeneity of their foundations. *Journal of Earthquake Engineering and Engineering Vibration***31:6**,167-173.

U.S. Atomic Energy Commission (1973), Regulatory Guide 1.60 “Design Response Spectra for Seismic Design of Nuclear Power Plants”

U.S. Nuclear Regulatory Commission (2007), NUREG-0800 “Review of Safety Analysis Reports for Nuclear Power Plants”